Journal of Saudi Chemical Society (2018) **22**, 372–379

King Saud University

Journal of Saudi Chemical Society

www.ksu.edu.sa
www.sciencedirect.com

ORIGINAL ARTICLE

Preparation of iron molybdate catalysts for methanol to formaldehyde oxidation based on ammonium molybdoferrate(II) precursor

N.V. Nikolenko [a], I.V. Kozhevnikov [b], A.O. Kostyniuk [c], H. Bayahia [d,*], Yu.V. Kalashnykov [a]

[a] *Department of General Chemical Technology, Ukrainian State University of Chemical Technology, Dnipropetrovsk, Gagarin Av., 8, 49005, Ukraine*
[b] *Department of Chemistry, University of Liverpool, Liverpool L69 7ZD, UK*
[c] *PetroSA Synthetic Fuels Innovation Centre, South African Institute for Advanced Materials Chemistry, University of the Western Cape, Cape Town, Private Bag X17, Bellville 7535, South Africa*
[d] *Department of Chemistry, Albaha University, Albaha, P.O. Box: 1988, 65431, Saudi Arabia*

Received 9 February 2016; revised 4 April 2016; accepted 5 April 2016
Available online 7 May 2016

KEYWORDS

Iron molybdate catalyst;
Ammonium molybdoferrate (II);
Methanol oxidation;
Formaldehyde

Abstract It was demonstrated that iron molybdate catalysts for methanol oxidation can be prepared using Fe(II) as a precursor instead of Fe(III). This would allow for reduction of acidity of preparation solutions as well as elimination of Fe(III) oxide impurities which are detrimental for the process selectivity. The system containing Fe(II) and Mo(VI) species in aqueous solution was investigated using UV–Vis spectroscopy. It was demonstrated that three types of chemical reactions occur in the Fe(II)–Mo(VI) system: (i) formation of complexes between Fe(II) and molybdate(VI) ions, (ii) inner sphere oxidation of coordinated Fe(II) by Mo(VI) and (iii) decomposition of the Fe–Mo complexes to form scarcely soluble Fe(III) molybdate, Mo(VI) hydrous trioxide and molybdenum blue. Solid molybdoferrate(II) prepared by interaction of Fe(II) and Mo(VI) in solution was characterized by EDXA, TGA, DTA and XRD and a scheme of its thermal evolution proposed. The iron molybdate catalyst prepared from Fe(II) precursor was tested in methanol-to-formaldehyde oxidation in a continuous flow fixed-bed reactor to show similar activity and selectivity to the conventional catalyst prepared with the use of Fe(III).

* Corresponding author.
E-mail address: n_nikolenko@ukr.net (N.V. Nikolenko).
Peer review under responsibility of King Saud University.

ELSEVIER Production and hosting by Elsevier

1. Introduction

Formaldehyde is the simplest and most important aldehyde, with world consumption of over 42 m tonnes, which is mainly applied in the production of urea- and phenol-formaldehyde resins. Formaldehyde is manufactured by selective catalytic

http://dx.doi.org/10.1016/j.jscs.2016.04.002
1319-6103

oxidation of methanol on an oxide catalyst. As the catalyst, a mixture of iron(III) molybdate and molybdenum(VI) oxide with a molar ratio Mo/Fe = 2–5 is most commonly used. This catalyst is considered to be one of the best since it allows for carrying out the oxidation process at relatively low temperatures and obtaining the high-concentration formaldehyde with low methanol and formic acid content. Despite the industrial success, work on further catalyst improvement is continued [1–12].

Iron(III) molybdate is usually prepared by precipitation from concentrated solutions of an iron(III) salt and molybdate [8–10]. However, the catalyst thus prepared is contaminated with iron(III) oxide as the individual phase which reduces the selectivity of methanol oxidation. It is well established that high selectivity performance of iron(III) molybdate is in contrast to the selectivity performance of Fe_2O_3, which shows essentially zero selectivity across the temperature range 200–400 °C and the dominant product is always CO_2 [9,11,13,14]. In order to remove the iron oxide a long (up to 48 h) heat treatment of catalyst precursor at 500 °C is required [9,10]. The solid-phase reactions proceeding between oxides of iron (III) and molybdenum(VI) upon annealing result in removal of impurities of iron oxide compounds from the catalyst [3]. Evidently, to reduce the cost of this stage of the synthesis, the content of impurities of iron oxide compounds must be minimal even at the stage of the iron molybdate deposition.

Thus, the main disadvantage of known preparation method is the use of highly acidic (pH $\leqslant$ 2) solutions of Fe(III) as well as the energy intensive catalyst annealing. Here, to overcome these disadvantages, we attempt the preparation of iron molybdate catalyst using Fe(II) salts instead of Fe(III). In aqueous solution, Fe^{2+} ion is more stable towards hydrolysis than Fe^{3+}. Therefore, less acidic Fe(II) solutions can be used for catalyst preparation. Subsequent air calcination of the Fe(II) molybdate thus obtained together with excess of MoO_3 will cause oxidation of Fe(II) to Fe(III) to afford a homogeneous mixture of Fe(III) molybdate and MoO_3 to be used as the catalyst for methanol oxidation. Here we also investigate chemical transformations involving Fe(II), Fe(III) and Mo(VI) in aqueous solutions in a wide range of pH using UV–Vis spectroscopy to determine equilibria in these systems. Solids precipitated in these systems are characterized by EDXA, TGA, DTA and XRD. The Fe–Mo catalysts prepared are tested in methanol oxidation using a continuous flow fixed-bed reactor.

2. Experimental

2.1. Chemicals used

Reagents that have been used in the preparation of catalysts and the catalytic reaction. Iron(III) nitrare nonahydrate (Sigma–Aldrich, 98 + %), Iron(II) sulfate heptahydrate (Sigma–Aldrich, 99 + %), Ammonium molybdate tetrahydrate (Sigma–Aldrich, 99.98%), Nitric acid (Sigma–Aldrich, 70%), Sulfuric acid (Sigma–Aldrich, 95–98%), Ammonia hydroxide solution (Sigma–Aldrich, 28–30% NH_3 basis), Methanol (Sigma–Aldrich, 99.8%).

2.2. Catalyst preparation

The preparation of Fe–Mo catalyst based on Fe(II) was carried out by gradual mixing of concentrated solutions of Fe (II) sulfate and ammonium heptamolybdate at room temperature (17 ± 2 °C) and a specified pH in the pH range of 5–6 with continuous stirring using a propeller stirrer (300 rpm). Reagent grade $FeSO_4{\cdot}7H_2O$ and $(NH_4)_6Mo_7O_{24}{\cdot}4H_2O$ and distilled water were used for catalyst preparation. The acidity of solutions was adjusted by 1 M H_2SO_4 and aqueous NH_4OH. To remove dissolved oxygen, prior to mixing, the solutions were flushed with nitrogen for 30 min. The resulting slurry was filtered using a Buchner funnel and the solid obtained was dried in a vacuum desiccator for further TGA, DTA and XRD investigations. For catalytic investigations the specimens of the dried solid was calcined at 500 °C for 5 and 48 h.

Catalyst preparation based on Fe(III) was carried out by adding drop-wise a concentrated solution of Fe(III) nitrate to a hot (~70 °C) solution of ammonium heptamolybdate acidified with nitric acid to pH 2 with continuous stirring. Fe (III) nitrate solution was prepared by dissolving the reagent grade $Fe(NO_3)_3{\cdot}9H_2O$ in 1 M HNO_3 solution. The resulting slurry was evaporated, oven dried at 110 °C and then calcined at 500 °C for 5 and 48 h.

2.3. Catalyst characterization

Fe–Mo solid materials were characterized by energy dispersive X-ray microanalysis (EDXA), TGA, DTA and XRD methods. The EDXA was carried out using a scanning electron microscope REMMA-102. The XRD was performed on a PANalytical X'Pert Pro diffractometer (monochromatic Cu-$K_{\alpha 1}$ radiation, λ = 1541 Å). The thermal analysis was performed on a differential scanning calorimeter Thermal Analysis Instruments SDT 2960 in the temperature range 20–600 °C in air flow (100 ml/min) with a heating rate of 10 °C/min. Temperatures above 600 °C were not investigated due to sublimation of Mo(VI) oxide. After heating, the sample was subjected to forced cooling at the same rate of 10 °C/min. On the DTA cooling curve no exo- or endothermic effects were observed which allowed using this curve as a base line when interpreting the DTA data.

2.4. Catalyst testing

The catalytic oxidation of methanol was performed in a continuous flow fixed-bed reactor with on-line GC analysis in the temperature range of 300–400 °C at ambient pressure. The catalyst testing setup had a U-shaped stainless steel tubular reactor of 9 mm internal diameter and a catalyst volume of 7.0 cm^3. The reactor was placed in a tubular furnace heated to a specified temperature within ± 5 °C. The temperature was controlled by a thermocouple, which was placed inside the reactor in the middle of the catalyst bed. To prevent temperature gradients the catalyst powder (1.5 g, 0.25–1 mm particle size) was mixed with a 4-fold excess of silicon carbide with the same particle size. The gas feed contained a mixture of methanol, O_2 and N_2 (3:20.3:75.7 by volume). The flow rate was controlled by calibrated rotameters within the range of contact times 0.01–0.035 min. Usually, the reaction reached steady state within 0.5 h. The mean absolute percentage error in conversion and selectivity was $\leqslant$10% and the carbon balance was maintained within 95%.

3. Results and discussion

3.1. Synthesis of ammonium molybdoferrate(II)

Mixing practically colourless aqueous solutions of Fe(II) sulfate and ammonium heptamolybdate at various Mo/Fe ratios was found to give quickly a black–brown solution containing Fe–Mo complexes. It is known that molybdate anions can form coordination compounds, e.g., heteropolyanions and isopolyanions, with many transition metal cations acting as mono- or polydentate ligands [15]. However, little data on Fe–Mo complexes are available in the literature. Therefore, we aimed to determine the composition and behaviour of such complexes. Initially it was assumed that with excess ammonium molybdate under appropriate reaction conditions (especially the Fe(II) and Mo(VI) concentration and pH) molybdoferrates of the $[Fe^{II}(OH)_m(Mo^{VI}O_4)_n]^z$ composition would form. Gravimetric and X-ray fluorescence analyses of fresh precipitates obtained in such systems confirmed the above assumption, as demonstrated in Fig. 1, which shows the Mo/Fe molar ratio in the precipitates obtained at different pH of the mother liquors. It can be seen that the Mo content in precipitates decreases linearly with increasing the pH of solutions (correlation factor $R^2 = 0{,}9303$). Extrapolation of this line to Mo/Fe = 6 indicates that molybdoferrate $[Fe^{II}(MoO_4)_6]^{10-}$ will be formed at pH < 4.5, whereas molybdenum free $Fe(OH)_2$ will be formed at pH > 7.

UV–Vis spectroscopic studies of molybdoferrate(II) solutions revealed three absorption bands at 880, 440 and 270 nm, which were not observed in the spectra of the Fe(II) and Mo(VI) solutions. For a d^6 transition metal cation such as Fe^{2+} in the weak octahedral crystal field, six d-d transitions from its ground state $^5T_{2g}$ are possible [16]. Therefore, the first low-intensity absorption band at 880 nm can be attributed to the electron transition $^5T_{2g} \rightarrow {}^5E_g(D)$. Is not possible to detect other d-d transitions in Fe^{2+} due to the presence of broad and intense absorption bands at 440 and 270 nm in the spectrum. Because of their high intensity these absorption bands could be attributed to the ligand-to-metal charge-transfer bands of the Fe–O and Mo–O bonds. These data suggest that interaction between Fe(II) and Mo(VI) species in solution results in formation of a complex with Fe(II) as the central atom and molybdate as the ligand.

Further it was found that over time even dilute solutions of Fe(II) molybdate become cloudy and gradually change their colour. Measuring UV–Vis absorbance showed that the intensity of the d–d transition at 880 nm was gradually increasing with time reaching a plateau in 15 min (Figs. 2 and 3). This may be explained by Fe(II) molybdate formation reaching equilibrium.

After 60 min, a reduction of the d-d transition intensity was observed followed by an increase in intensity after 70 min (Fig. 3). The intensity of the charge-transfer band at 440 nm was decreasing with time passing a minimum at about 65 min followed by an increase in intensity afterwards. This can be attributed to a continuous change in the composition of the Fe(II) molybdate complexes.

Our study of the Tyndall light scattering on the Fe–Mo solutions and the obedience of light absorption to the Geller empirical equation indicated that the initially true Fe–Mo solutions transformed to a sol in a few hours, with gradual colour change to light brown. The formation of colloidal particles in solution can be explained by oxidation of Fe(II) to Fe(III) by Mo(VI) and formation of poorly soluble Fe(III) molybdates.

The evolution of the UV–Vis spectra observed (Figs. 2 and 3) could be explained by inner sphere oxidation of Fe(II) by Mo(VI) (Eq. (1)). The formation of Mo(V) in these solutions was confirmed by reaction with thiocyanate ions yielding a coloured Mo(V)-thiocyanate complex (the test with thiocyanate was carried out in the presence of excess of fluoride ions masking Fe(III)). It should be noted that the UV–Vis spectroscopy failed to confirm the formation of Fe(III) and Mo(V) probably due to their weak d-d electron transitions, which are forbidden by the spin and Laporte selection rules for Fe(III) and Mo(V), respectively [16].

$$\left[Fe^{2+}\left(Mo^{VI}O_4^{2-}\right)_X\right] \rightleftarrows \left[Fe^{3+}\left(Mo^{VI}O_4^{2-}\right)_{X-1}\left(Mo^{V}O_4^{3-}\right)\right] \qquad (1)$$

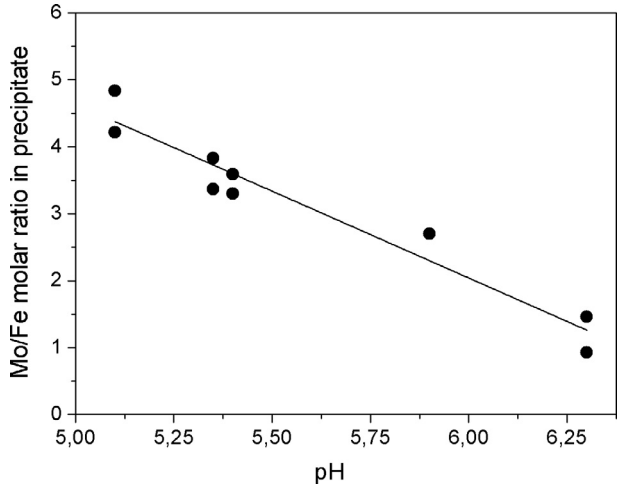

Figure 1 Mo/Fe molar ratio of Fe(II) molybdate precipitate as a function of pH of the mother liquor at the starting solution Mo/Fe molar ratio of 3:1.

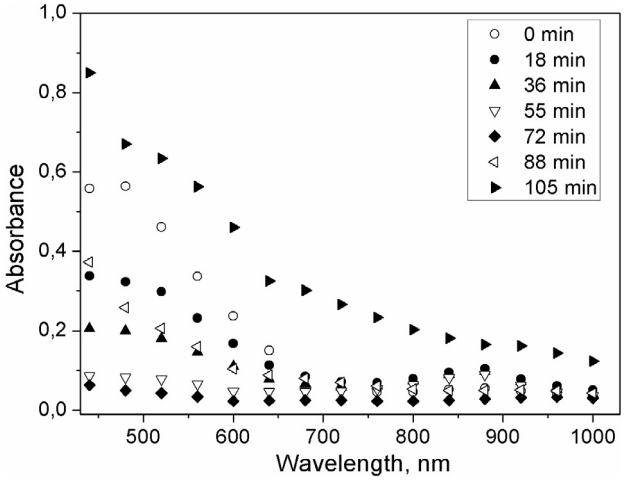

Figure 2 Evolution of UV–Vis spectra of Fe(II) molybdate solution prepared by mixing 0.1 M solutions of Fe(II) sulfate and ammonium heptamolybdate at a Mo/Fe molar ratio of 2:1 and pH 6.1.

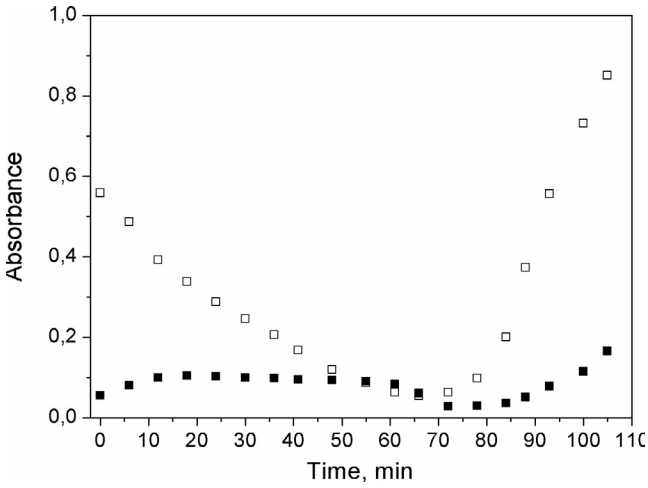

Figure 3 Evolution of UV–Vis absorption at 440 nm (open squares) and 880 nm (filled squares) of Fe(II) molybdate solution prepared by mixing 0.1 M solutions of Fe(II) sulfate and ammonium heptamolybdate (Mo/Fe = 2:1 and pH 6.1).

The equilibrium constant, K, of reaction (1) can be estimated approximately from Eq. (2), where ΔG^0 is the standard Gibbs free energy of reaction; n, the number of electrons transferred in the redox process; F, Faraday's constant; E^0, the standard cell potential.

$$\Delta G^0 = -\mathrm{RTlnK} = -nFE^0 \quad (2)$$

From the standard potentials of redox pairs Mo(VI)/Mo(V) and Fe(III)/Fe(II), it was calculated $\Delta G^0 = 28$ kJ/mol at pH 0, which corresponds to $K = 1.2{\cdot}10^{-5}$. Therefore, equilibrium (1) is shifted to the left. Nevertheless, the equilibrium concentrations of Fe(III) and Mo(V) could be $\sim 10^{-3}$ M in 1 M solution of Fe(II) and Mo(VI), which could cause the formation of the above mentioned colloidal particles.

To determine the dependence of K on the pH, the Pourbaix diagram of molybdenum and iron was used [17]. It was found that with increasing pH the K value decreases rapidly, reaching its lowest value of 10^{-9} at a pH 4.5. The dependence log$K$/pH has the form of five linear segments with kinks at pH values equal to the pK values corresponding to the formation of MoO_2OH^+, $FeOH^{2+}$, $Fe(OH)_2^+$ and $Fe(OH)_3$ species in solution. This is due to the fact that the change in pH of solution causes a change of the dominant forms of iron and molybdenum hydroxy complexes, affecting their redox potentials.

Calculation of equilibrium composition of Fe(II)–Mo(VI) solutions taking into account the effect of pH on equilibrium constants showed that in the pH range studied Fe(III) and Mo(V) ions will be present in solution in concentrations three to four orders of magnitude lower than those of Fe(II) and Mo (VI). Increasing the concentration of Fe(II) and Mo(VI) will increase the equilibrium concentrations of Fe(III) and Mo(V) as well to cause, at a certain concentration level, precipitation of Fe(III) molybdate, Fe(III) hydroxide and Mo(V) oxyhydroxide. Obviously, such reactions are responsible for the sol formation observed upon mixing of Fe(II) and Mo (VI) salts.

Solubility, S, of a sparingly soluble salt can be characterized by solubility diagrams showing the concentration of saturated solution as a function of acidity or the content of one of constituent ions. The log$S$ – pH solubility diagrams calculated for Fe(III) hydroxide and molybdate, molybdic acid, Fe(II) hydroxide and molybdate and Mo(V) oxyhydroxide are shown in Fig. 4. Due to the lack of reference data, the solubility products of some compounds were calculated from our experimental data on the concentrations of saturated solutions at 17 ± 2 °C. Best agreement between the experimental and calculated data for the logS – pH solubility diagrams were obtained at the following values of solubility products: $2{\cdot}10^{-8}$ ($Fe^{II}MoO_4$), 10^{-13} ($MoO_3{\cdot}nH_2O$), 10^{-15} ($MoO_2(OH)$) and 10^{-50} ($Fe_2(MoO_4)_3$).

According to the data shown in Fig. 4, deposition of Fe(II) molybdate is possible only within the pH range of 4.5–8. In more acidic or alkaline solutions, thermodynamically favoured solid phases are $MoO_3{\cdot}nH_2O$ and $Fe(OH)_2$, respectively. The equilibrium concentration of Mo(V) produced by reduction of Mo(VI) with Fe(II) in their 1 M solution is about an order of magnitude less than the solubility of Mo(V) oxyhydroxide. Therefore, in such conditions, $MoO_2(OH)$ will not precipitate. This is, however, only a preliminary conclusion because the equilibrium concentration of Fe(III) greatly exceeds the solubility of Fe(III) molybdate in the pH range under consideration. Therefore, the Fe(III) ions, as they emerge, will precipitate as Fe(III) molybdate, which will shift equilibrium (1) to the right to increase the concentration of MoO_2^+ ions in solution. When the MoO_2^+ concentration reaches the $MoO_2(OH)$ solubility, it will precipitate as well, shifting equilibrium (1) further to the right. It should be noted, however, that competing reaction of MoO_2^+ with MoO_4^{2-} could occur resulting in formation of molybdenum blue, an isopoly compound of variable composition containing Mo(VI) and Mo (V) [18].

Therefore, as $Fe_2(MoO_4)_3$, $MoO_2(OH)$ and molybdenum blue precipitate, the conversion of Fe(II) to Fe(III) will continuously increase. This means that "true" equilibrium in the Fe (II)–Mo(VI) system is set up only when a balance between Fe (II) oxidation and Fe(III) molybdate solubility is reached.

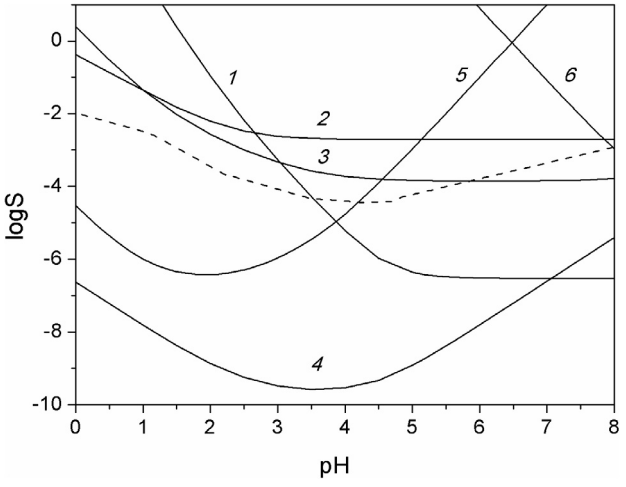

Figure 4 Solubility of $Fe(OH)_3$ (1), $MoO_2(OH)$ (2), $FeMoO_4$ (3), $Fe_2(MoO_4)_3$ (4), $MoO_3{\cdot}nH_2O$ (5) and $Fe(OH)_2$ (6) in aqueous solution at room temperature (dashed line shows the logarithm of equilibrium concentrations of Fe(III) and Mo(V) formed by mixing 1 M solutions of Fe(II) and Mo(VI) at a Mo/Fe molar ratio of 2:1).

3.2. TGA and DTA study of ammonium molybdoferrate(II)

Fig. 5 shows the TGA and DTA results for ammonium molybdoferrate(II) with a molar ratio of Mo/Fe = 2.2. The weight loss is 19.5% upon heating to 600 °C, most of it between room temperature and 150 °C. The DTA shows that the thermal transformation involves both endothermic (at 93, 126 and 247 °C) and exothermic (360, 386 and 425 °C) effects. The weight loss up to 100 °C and the endothermic effect at 93 °C may be attributed to the loss of physisorbed water. The endothermic effect at 126 °C may be the result of ammonium molybdoferrate decomposition to form Fe(II) molybdate phase in accordance with Eq (3). Evolution of ammonia in this stage was confirmed experimentally by heating the sample in a test tube at 120–150 °C and absorbing of the ammonia evolved in a water trap, from which the ammonia was determined using the Nessler's reagent.

$$((NH_4)_xH_y[Fe^{II}(MoO_4)_z] \rightarrow FeMoO_4 + (z-1)MoO_3 + yH_2O + xNH_3 \quad (3)$$

Liberation of ammonia was also detected on heating ammonium molybdoferrate at 250 °C. In the DTA/TGA (Fig. 5), the endothermic effect at 248 °C is characterized by a weight loss of only 3.0%. This may indicate that it is due to decomposition of an impurity, most likely ammonium sulfate to form ammonium hydrogensulfate (Eq. (4)).

$$(NH_4)_2SO_4 \rightarrow NH_4HSO_4 + NH_3 \quad (4)$$

There is a small endothermic effect at 325–350 °C, which is masked by a large exothermic effect at 360 °C. The TGA also shows a weight loss at 340 °C in this temperature range. This may be attributed to the precursor ammonium molybdate impurity present in the sample. Ammonium molybdate is known to decompose in the temperature range of 325–350 °C [19]: $(NH_4)_xMo_yO_z \rightarrow yMoO_3 + xNH_3 + nH_2O$.

The exothermic effect at 360 °C may be associated with oxidation of Fe(II) ions in the $FeMoO_4$ phase by O_2. Weight gain, which accompanies this exothermic effect, supports this assumption. Oxidation of Fe(II) in the presence of ammonium sulfate in air has been studied by Mössbauer spectroscopy [20] to reveal that it begins above 150 °C, reaching the maximum rate at 360 °C, which agrees well with our TGA/DTA data. The oxidation of $FeMoO_4$ to $Fe_2(MoO_4)_3$ (Eq. (5)) was confirmed by XRD (see below).

$$2FeMoO_4 + MoO_3 + 1/2O_2 \rightarrow Fe_2(MoO_4)_3 \quad (5)$$

The exothermic effect at 390 °C is likely to occur due to decomposition of ammonium hydrogensulfate to form ammonium pyrosulfate: $2NH_4HSO_4 \rightarrow (NH_4)_2S_2O_7 + H_2O$ [21,22]. The exothermic peak at 400–440 °C may be explained by the decomposition of ammonium pyrosulfate (Eq. (6)) [23,24].

$$3(NH_4)_2S_2O_7 + 2Fe_2(MoO_4)_3 \rightarrow 2Fe_2(SO_4)_3 + 6MoO_3 + 6NH_3 + 3H_2O \quad (6)$$

The last endothermic effect at 425 °C accompanied by weight loss can be attributed to decomposition of Fe(III) sulfate: $Fe_2(SO_4)_3 \rightarrow Fe_2O_3 + 3SO_2 + 1.5O_2$ [25].

The proposed scheme of thermal behaviour of molybdoferrate(II) must be supplemented by reactions between Fe and Mo oxides. It was found that complete conversion of ammonium molybdoferrate(II) into the mixture of Fe(III) molybdate and MoO_3 phases occurred after prolonged annealing of the test samples at temperatures of 500–600 °C. This must involve solid-phase interaction between Fe(III) and Mo(VI) oxides to form Fe(III) molybdate: $Fe_2O_3 + 3MoO_3 \rightarrow Fe_2(MoO_4)_3$ [2,3]. The absence of DTA thermal effect for this reaction is likely due to a low content of Fe_2O_3 in the sample studied.

3.3. XRD study of ammonium molybdoferrate(II)

This study aimed at determining phase composition of ammonium molybdoferrate(II) obtained by precipitation from Fe–Mo solutions as well as phase composition of products obtained by heat treatment of ammonium molybdoferrate(II).

Fig. 6 shows the XRD for ammonium molybdoferrate(II) precipitated at Mo/Fe molar ratio of 2.2 and dried under vacuum at room temperature. It displays a crystal pattern with peaks at 8.0, 10.0, 11.2, 15.3, 16.1, 17.4, 18.1 and 29.0 degrees. Our search in the ICDD PDF-2 database gave no results for this sample.

The most intense peaks were close to the compound $(NH_4)_3H_6[Fe^{III}(Mo^{VI}O_4)_6]$ (ICDD PDF-2, 00-004-0610), but

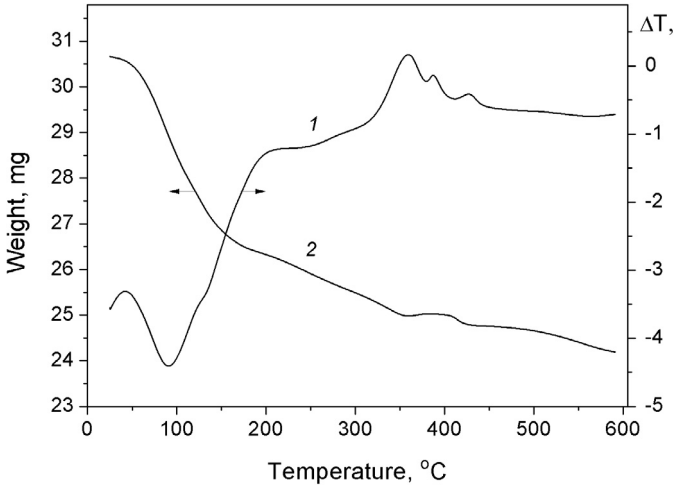

Figure 5 DTA (1) and TGA (2) of ammonium molybdoferrate(II) (Mo/Fe = 2.2, 100 ml/min air flow rate, 10 °C/min heating rate).

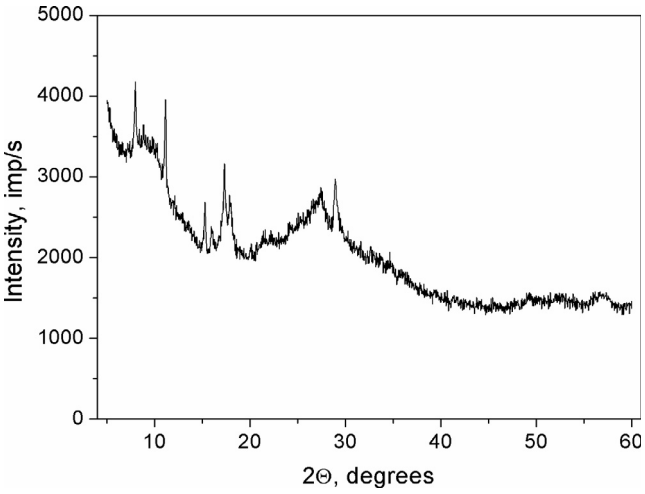

Figure 6 XRD of ammonium molybdoferrate(II) precipitated at Mo/Fe molar ratio of 2.2 and dried under vacuum at room temperature.

the intensity and position of other peaks were somewhat different from the diffraction pattern of our sample. This difference may be explained by the fact that the central atom in our sample is Fe(II) rather than Fe(III) in the reference compound. Also the number of molybdate ligands may be different in the two samples.

Fig. 7 presents the XRD for ammonium molybdoferrate(II) pre-heated in air at temperatures corresponding to the weight losses observed by TGA (Fig. 5), namely 140, 240, 340 and 366 °C (10 °C/min heating rate). It can be seen that the heat pre-treatment from 140 to 240 °C significantly reduced sample crystallinity, which can be explained by decomposition of ammonium molybdoferrate(II) crystal structure due to reaction (3).

After pre-treatment at 340 °C, peaks of Fe(III) molybdate (2θ = 20.4, 22.9, 25.9 and 27.3 degrees) appear. After pre-treatment 366 °C, besides Fe(III) molybdate, peaks of MoO_3 (2θ = 12.8, 25.7, 27.4 and 33.8 degrees) and those of Fe(II) molybdate (2θ = 15.3, 25.0, 25.6 and 30.1 degrees) are observed. Therefore, the XRD data obtained confirm the proposed scheme of chemical transformations of ammonium molybdoferrate(II).

In result of a detailed computer-assisted XRD analysis of the molybdoferrate(II) samples after calcination at 500 °C for 1–10 h it was found that the time taken for the complete conversion of Fe_2O_3 impurity to $Fe_2(MoO_4)_3$ is no shorter than 5 h.

3.4. Catalyst testing in methanol oxidation

Kinetics and mechanism of selective oxidation of methanol on iron molybdate catalysts has been addressed in previous reports ([8–10] and references therein). In this work, we compared the iron molybdate catalysts prepared using Fe(III) and Fe(II) precursors regarding their activity and selectivity in methanol-to-formaldehyde oxidation in a continuous flow fixed-bed reactor at temperatures 300 °C. Both catalysts had an industrial Mo/Fe molar ratio of 2.2 and were calcined at 500 °C for 5 and 48 h [8–10].

It was found that for both catalysts the reaction of partial oxidation of methanol obeyed the Arrhenius equation with apparent activation energy of 64 kJ/mol. This value is in reasonable agreement with an estimate of 70–90 kJ/mol [26] and indicates that the reaction of partial oxidation of methanol was not affected by diffusion limitations.

Catalysts prepared using Fe(III) precursor and calcined at 500 °C for 5 h showed the worst formaldehyde selectivity (Fig. 8). Its selectivity remained at a constant level of 95% only up to 50–60% methanol conversion followed by a sharp decline at higher methanol conversions. This trend is in good agreement with the previous reports [8,9]. Contrariwise, catalysts prepared using Fe(II) precursor and calcined at 500 °C for 5 h showed the best formaldehyde selectivity. Its selectivity remained at a constant level of 95% up to 95% methanol conversion and coincided with selectivity of catalysts which were prepared using as Fe(II) and Fe(III) precursors with calcination at 500 °C for 48 h.

These results show that calcination at 500 °C for 5 h is insufficient for catalyst based on Fe(III) precursor and a long

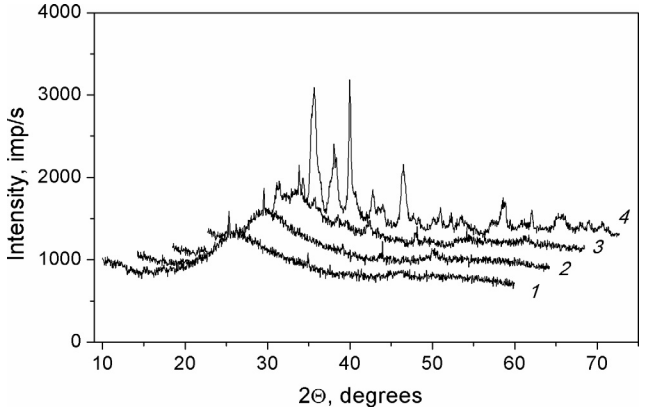

Figure 7 XRD of ammonium molybdoferrate(II) heated in air at different temperatures: (1) 140 °C, (2) 240 °C, (3) 340 °C and (4) 366 °C.

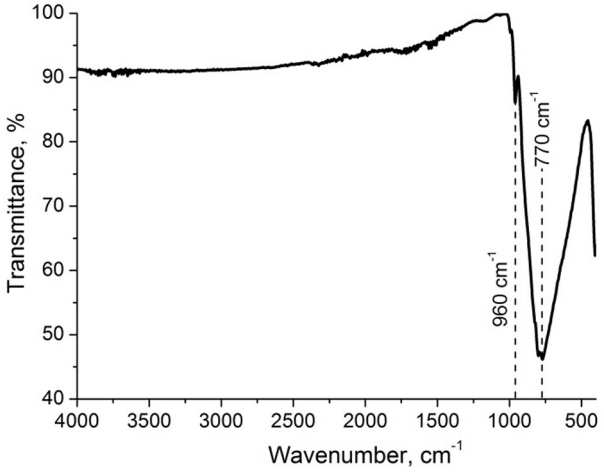

Figure 8 FTIR spectra of the precipitate obtained by continuous crystallization at Mo/Fe = 2.2 and calcined at 500 °C.

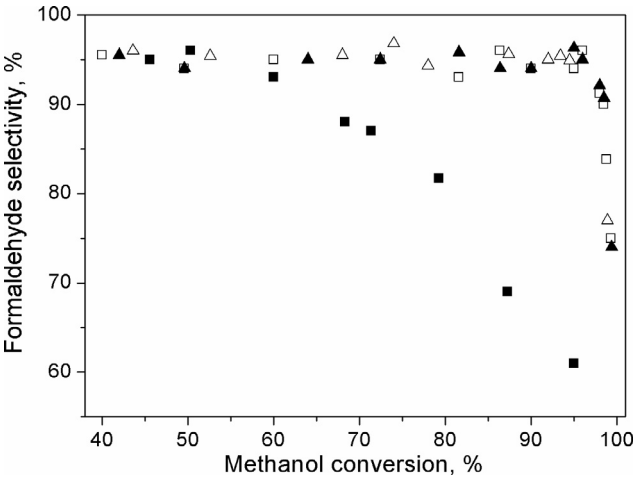

Figure 9 Formaldehyde selectivity versus methanol conversion for methanol oxidation at 300 °C on iron molybdate catalysts an Mo/Fe molar ratio of 2.2 prepared from Fe(III) (filled squares for 5 h and filled triangles for 48 h calcination at 500 °C) and Fe(II) (open squares for 5 h and open triangles for 48 h calcination at 500 °C).

(up to 48 h) heat treatment is required. The preparation of iron molybdate catalyst using Fe(II) as a precursor reduces the cost of the synthesis and gives the catalyst whose performance in methanol oxidation fully matches the performance of the conventional catalyst prepared with the use of Fe(III) (see Fig. 9).

4. Conclusions

It has been demonstrated that iron molybdate catalysts for methanol oxidation can be prepared using Fe(II) as a precursor instead of Fe(III), which would allow for reduction of acidity of preparation solutions as well as elimination of Fe(III) oxide impurities which are detrimental for the process selectivity. It has also been demonstrated that three types of chemical reactions occur in the Fe(II)–Mo(VI) system: (i) formation of complexes between Fe(II) and molybdate(VI) ions, (ii) inner sphere oxidation of coordinated Fe(II) by Mo(VI) and (iii) decomposition of the Fe–Mo complexes to form scarcely soluble Fe(III) molybdate, Mo(VI) hydrous trioxide and molybdenum blue. Solid molybdoferrate(II) prepared by interaction of Fe(II) and Mo(VI) in solution has been characterized by EDXA, TGA, DTA and XRD and a scheme of its thermal evolution proposed. The iron molybdate catalyst prepared using Fe(II) precursor has been tested in methanol-to-formaldehyde oxidation in a continuous flow fixed-bed reactor. Its performance in methanol oxidation has been found to fully match the performance of the conventional catalyst prepared with the use of Fe(III) regarding their activity and selectivity.

Acknowledgments

The authors would like to thank Ministry of Education and Science of Ukraine and Albaha University of Saudi Arabia for financial supports.

References

[1] A.P.V. Soares, M. Fatima, M.F. Portela, A. Kiennemann, The role of the suprastoichiometric molybdenum during methanol to formaldehyde oxidation over Mo–Fe mixed oxides, J. Mol. Catal. A Chem. 397 (2015) 93–98.
[2] M.V. Nikolenko, A.O. Kostynyuk, F. Goutenoire, Y.V. Kalashnikov, Chemical precipitation of iron(III) molybdate + molybdenum trioxide mixtures through continuous crystallization, Inorg. Mater. 50 (2014) 1140–1145.
[3] A.O. Kostynyuk et al, Kinetics of the thermal treatment of an iron–molybdenum catalyst, Kinet. Catal. 55 (2014) 649–655.
[4] G. Jin et al, $Fe_2(MoO_4)_3/MoO_3$ nano-structured catalysts for the oxidation of methanol to formaldehyde, J. Catal. 296 (2012) 55–64.
[5] W. Zhou et al, Origin of the synergistic interaction between MoO_3 and iron molybdate for the selective oxidation of methanol to formaldehyde, J. Catal. 275 (2010) 84–98.
[6] A. Beale et al, An iron molybdate catalyst for methanol to formaldehyde conversion prepared by a hydrothermal method and its characterization, Appl. Catal. A Gen. 363 (2009) 143–152.
[7] A.P.S. Dias, A. Rozanov, J. Waerenborgh, M. Portela, New Mo–Fe–O silica supported catalysts for methanol to formaldehyde oxidation, Appl. Catal. A Gen. 345 (2008) 185–194.
[8] M.P. House, A.F. Carley, R. Echeverria-Valda, M. Bowker, Effect of varying the cation ratio within iron molybdate catalysts for the selective oxidation of methanol, J. Phys. Chem. C 112 (2008) 4333–4341.
[9] M. Bowker et al, The selective oxidation of methanol on iron molybdate catalysts, Top. Catal. 48 (2008) 158–165.
[10] M.P. House, M.D. Shannon, M. Bowker, Surface segregation in iron molybdate catalysts, Catal. Lett. 122 (2008) 210–213.
[11] A. Andersson, M. Hernelind, O. Augustsson, A study of the ageing and deactivation phenomena occurring during operation of an iron molybdate catalyst in formaldehyde production, Catal. Today 112 (2006) 40–44.
[12] A.P.V. Soares, M.F. Portela, A. Kiennemann, L. Hilaire, Mechanism of deactivation of iron-molybdate catalysts prepared by coprecipitation and sol–gel techniques in methanol to formaldehyde oxidation, Chem. Eng. Sci. 58 (2003) 1315–1322.
[13] N.V. Nikolenko, A.O. Kostynyuk, Y.V. Kalashnikov, E.A. Cheremis, The Calculation of the thermodynamic equilibrium in the system $Fe^{3+}/MoO_4^{2-}/H^+(OH^-)/H_2O$ and determination of the reasonable conditions for the deposition of iron molybdate, Russ. J. Appl. Chem. 85 (2012) 1814–1819.
[14] M. Bowker, Rules for selective oxidation exemplified by methanol selective oxidation on iron molybdate catalysts, Top. Catal. 58 (2015) 606–612.
[15] M.T. Pope, Heteropoly and Isopoly Oxometallates, Springer-Verlag, Berlin, 1983.
[16] I.B. Bersuker, Electronic structure and properties of transition metal compounds: introduction to the theory, Wiley, New York, 1996.
[17] Atlas of Eh–pH diagrams. Intercomparison of thermodynamic database (2005) Geological Survey of Japan open file report No 419. National Institute of Advanced Industrial Science and Technology, research center for Deep Geological Environment, Naoto Takeno.
[18] I.A. Weinstock, Homogenous-phase electron-transfer reactions of polyoxometalates, Chem. Rev. 98 (1998) 113–170.
[19] W.M. Shaheen, Thermal behaviour of pure and binary Fe $(NO_3)_3{\cdot}9H_2O$ and $(NH_4)_6Mo_7O_{24}{\cdot}4H_2O$ systems, Mater. Sci. Eng. A 2006 (445–446) (2006) 113–121.

[20] E. Frank, M.C. Varriale, A. Bristoti, Mossbauer studies of the thermal decomposition of iron(II) ammonium sulfate hexahydrate, J. Therm. Anal. 17 (1979) 141–150.
[21] R. Kiyoura, K. Urano, Mechanism, kinetics, and equilibrium of thermal decomposition of ammonium sulfate, Ind. Eng. Chem. Proc. Design Dev. 9 (1970) 489–494.
[22] L. Jing-Hua, Z. Gui-En, Investigation of the kinetics and mechanism of decomposition of ammonium hydrogen sulfate, Acta Phys. Chim. Sin. 8 (1992) 123–127.
[23] X. Song et al, Thermal decomposition mechanism of ammonium sulfate catalyzed by ferric oxide, Front. Chem. Sci. Eng. 7 (2013) 210–217.
[24] T. Nagaishi, S. Ishiyarna, M. Matsumoto, S. Yoshinaga, Reactions between ammonium sulfate and metal oxides (metal = Cr, Mn and Fe) and thermal decomposition of the products, J. Therm. Anal. 29 (1984) 121–129.
[25] J. Straszko, M. Olszak-Humienik, J. Mozejko, The kinetic parameters of thermal decomposition hydrated iron sulfate, J. Therm. Anal. 48 (1996) 1415–1422.
[26] A. Kostynyuk, M. Nikolenko, Iron molybdate catalyst stabilized by calcium oxide for methanol to formaldehyde conversion, Chem. Chem. Technol. 5 (2011) 89–95.